European Journal of Chemistry

View Journal Online
View Article Online

Synthesis, crystal structure, Hirshfeld surface and interaction energies analysis of 3-(benzo[*d*][1,3]dioxol-5-yl)-2-(pyridin-3-yl)thiazolidin-4-one

Summara Kousar [1], Raed Al-Qawasmeh [2,3], Monther Khanfar [2,3] and Muhammad Saeed [1,*]

[1] *Department of Chemistry and Chemical Engineering, Syed Babar Ali School of Science and Engineering, Lahore University of Management Sciences, Lahore, 54792, Pakistan*
[2] *Department of Chemistry, College of Sciences, University of Sharjah, Sharjah, 27272, United Arab Emirates*
[3] *Department of Chemistry, University of Jordan, Amman, 11942, Jordan*

* *Corresponding author at: Department of Chemistry and Chemical Engineering, Syed Babar Ali School of Science and Engineering, Lahore University of Management Sciences, Lahore, 54792, Pakistan.*
e-mail: muhammad.saeed@lums.edu.pk (M. Saeed).

RESEARCH ARTICLE

10.5155/eurjchem.17.2.99-108.2778

Received: 16 January 2026
Received in revised form: 3 April 2026
Accepted: 17 April 2026
Published online: 30 June 2026
Printed: 30 June 2026

KEYWORDS

Synthesis
Hirshfeld surfaces
Interaction energies
X-ray crystallography
1,3-Thiazolidin-4-one
Supramolecular features

ABSTRACT

3-(Benzo[*d*][1,3]dioxol-5-yl)-2-(pyridin-3-yl)thiazolidin-4-one, a novel derivative of 1,3-thiazolidin-4-one, was synthesized by Schiff base formation followed by cyclocondensation with thioglycolic acid. The structure of the synthesized compound was characterized by spectroscopic techniques, including NMR, GC-MS, and HRMS. The molecular structure was unambiguously established by single-crystal X-ray diffraction. The compound crystallizes in the monoclinic crystal system with space group *C*2/*c (No. 15) and* unit-cell parameters a = 14.69 Å, b = 9.615 Å, c = 22.198 Å, and β = 98.49°. The molecular geometry reveals that the sulfur atom of the 1,3-thiazolidin-4-one ring is significantly out of the plane of the remaining ring atoms and adopts a puckered conformation. In the solid state, the supramolecular architecture is stabilized by a combination of interactions, including hydrogen bonding and weak π···π interactions. Furthermore, Hirshfeld surface analysis and two-dimensional fingerprint plots were used to quantify the intermolecular interactions, revealing that H···H (32.4%), O···H/H···O (20.2%) C···H/H···C (18.1%) contacts make the most significant contribution to Hirshfeld surfaces. Energy framework calculations indicated that dispersion energy, arising mainly from π···π interactions, is the dominant contributor to stabilization of the crystal packing.

Cite this: *Eur. J. Chem.* **2026**, *17(2)*, 99-108 **Journal website**: www.eurjchem.com

1. Introduction

Heterocyclic compounds containing heteroatoms, mainly nitrogen, oxygen, and sulfur, have been widely recognized for their diverse biological profiles and are therefore under hot pursuit by medicinal chemists [1]. Among them, 1,3-thiazolidin-4-one is an important heterocyclic motif that contains one sulfur atom and one nitrogen atom in a five-membered ring at positions 1 and 3 with a carbonyl group at position 4 [2,3]. Due to its remarkable biological versatility, 4-thiazolidinone is considered a "magic moiety" and exhibits a wide spectrum of biological activities, including antimicrobial [4], anti-inflammatory [5,6], leishmanicidal or trypanocidal [7,8], antidiabetic [9,10], antiviral [11], anti-HIV [12], antibacterial [13,14], cardiovascular [15], antitumor [11,16,17], anti-histaminic, anti-convulsant, and antitubercular activities [18].

The biological activity of a compound is strongly influenced by the spatial orientation of the groups attached at different positions and by the intermolecular forces involved in interactions with biological systems. This information can be obtained accurately from a solid-state structural analysis using single-crystal X-ray diffraction [19,20].

Our group has been working on the synthesis and biological evaluation of novel heterocyclic scaffolds [21,22]. As part of our ongoing efforts, we became interested in the design and synthesis of new 1,3-thiazolidin-4-one derivatives to explore their biological activities and structure-activity relationships. Interestingly, a novel derivative was successfully crystallized, prompting us to analyze its crystal structure using X-ray crystallography. Here, we report the synthesis and crystallographic data of 3-(benzo[*d*][1,3]dioxol-5-yl)-2-(pyridin-3-yl)thiazolidin-4-one, together with Hirshfeld surface analysis, two-dimensional fingerprint analysis, and interaction energy calculations that may be relevant to its biological behavior.

2. Experimental

2.1. Materials

All chemicals and solvents used in the synthesis were of analytical grade from Sigma Aldrich and were used without further purification. The solvents for column chromatography were distilled before use. Silica gel (pore size 60 Å, 40-63 mm, 230-400 mesh size) was used for chromatographic purification

https://dx.doi.org/10.5155/eurjchem.17.2.99-108.2778

Table 1. Crystal data and structure refinement for 3-(benzo[*d*][1,3]dioxol-5-yl)-2-(pyridin-3-yl)thiazolidin-4-one.

Parameters	Compound 5
Empirical formula	$C_{20}H_{15}NOS$
Formula weight	317.39
Temperature [K]	100(2)
Crystal system	Monoclinic
Space group (number)	*C*2/*c* (15)
a [Å]	14.690(9)
b [Å]	9.615(5)
c [Å]	22.198(15)
β [°]	98.49(3)
Volume [Å^3]	3101(3)
Z	8
ρ_{calc} [gcm^{-3}]	1.360
μ [mm^{-1}]	0.212
F(000)	1328
Crystal size [mm^3]	0.077×0.109×0.242
Crystal colour	clear colourless
Crystal shape	block
Radiation	MoK_α (λ=0.71073 Å)
2θ range [°]	3.71 to 53.46 (0.79 Å)
Index ranges	$-18 \le h \le 18$, $-12 \le k \le 10$, $-28 \le l \le 25$
Reflections collected	10275
Independent reflections	3279, R_{int} = 0.1003, R_{sigma} = 0.1325
Completeness to θ = 25.242°	99.8
Data / Restraints / Parameters	3279 / 0 / 209
Absorption correction T_{min}/T_{max} (method)	0.950 / 0.984 (Multi-Scan)
Goodness-of-fit on F^2	1.006
Final R indexes [I≥2σ(I)]	R_1 = 0.0691 wR_2 = 0.1431
Final R indexes [all data]	R_1 = 0.1488 wR_2 = 0.1934
Largest peak/hole [eÅ^{-3}]	0.56/−0.60
Extinction coefficient	0.0138(11)

Precoated silica gel TLC plates were used to monitor the progress of the reaction, and spots were visualized under a 254 nm UV lamp. The melting point was determined on a digital melting point apparatus (STUART SMP3) and is uncorrected. The ^{1}H and ^{13}C NMR spectra were recorded on a 600 MHz Bruker Avance Neo NMR instrument (150 MHz for ^{13}C) using deuterated chloroform ($CDCl_3$) as the solvent. Chemical shifts are reported in δ values (ppm) with reference to the solvent used. The abbreviations s(singlet), d (doublet), t (triplet), dd (doublet of doublet), dt (doublet of triplet), and m (multiplet) are used. GCMS analyses were performed on a 1300 GC-MS instrument (Thermo Scientific). HRMS data were acquired on the MS instrument equipped with an electron spray ionization (ESI) source and a time-of-flight (TOF) detector.

2.2. Synthesis of 3-(benzo[d][1,3]dioxol-5-yl)-2-(pyridin-3-yl)thiazolidin-4-one (5)

To a stirred solution of pyridine-3-carbaldehyde (1) (1 mmol) and benzo[*d*][1,3]dioxol-5-amine (**2**) (1 mmol) in DCM (5 mL) 600 mg Na_2SO_4 was added at room temperature. The reaction mixture was stirred for 5-6 h (TLC control). The reaction mixture was then filtered and evaporated to obtain crude Schiff base (3), which was reconstituted in 5 mL of toluene, and thioglycolic acid (4) (2 mmol) was added. The reaction mixture was refluxed for 16 h. The advancement of the reaction was monitored by thin-layer chromatography (TLC). The crude product obtained was purified by column chromatography using n-hexane and ethyl acetate (7:3) as a mobile phase. The title compound was recrystallized in ethyl acetate/hexane (3:7) by slow evaporation at room temperature to obtain a shiny, colorless crystalline solid with 86% yield. M.p.: 158-160 °C. ^{1}H NMR (600 MHz, $CDCl_3$, δ, ppm): 8.54 (dd, *J* = 4.9, 1.6 Hz, 1H, H13), 8.52 (d, *J* = 2.4 Hz, 1H, H12), 7.80 (dt, *J* = 8.0, 2.0 Hz, 1H, H14), 7.35 (dd, *J* = 8.4, 5.3 Hz, 1H, H15), 6.67 (d, *J* = 8.3 Hz, 1H, H4), 6.60 (d, *J* = 2.1 Hz, 1H, H7), 6.52 (dd, *J* = 8.3, 2.1 Hz, 1H, H5), 6.03 (d, *J* = 2.1 Hz, 1H, H8), 5.93-5.88 (m, 2H, H2A, H2B), 3.97 (dd, *J* = 15.8, 1.8 Hz, 1H, H9B), 3.90 (d, *J* = 15.9 Hz, 1H, H9A). ^{13}C NMR (151 MHz, $CDCl_3$, δ, ppm): 170.76, 149.31, 148.35, 147.81, 147.14, 136.25, 135.72, 130.32, 124.27, 119.93, 108.54, 107.64, 101.78, 63.31, 33.31. MS (EI, *m/z* (%)) calcd. for $C_{15}H_{12}N_2O_3S$, $[M]^+$ 300.33. GC-MS (EI, *m/z* (%)): 302.02 (M+2, 04%), 301.04 (M+1, 16%), 299.98 (M^+, 100%), 227.13 (12%), 226.19 (32%), 167.00 (62%), 136.10 (80%). HRMS (EI, *m/z*) calcd. for $C_{15}H_{12}N_2O_3S$ $([M+H])^+$ 301.0647; found 301.0633.

2.3. Single-crystal X-ray diffraction data collection

A clear, colorless block-shaped crystal of compound 5 was mounted on a goniometer. A Bruker D8 VENTURE FIXED CHI diffractometer was used for curation of single-crystal XRD data. The diffractometer was equipped with a monochromator (a microfocus sealed tube using a multilayer mirror), a Bruker PHOTON III CPAD detector, and an Oxford Cryostream 1000 low-temperature device. The radiation source was Mo K_α (λ = 0.71073 Å). All data were integrated with SAINT V8.40B, generating 10275 reflections, of which 3279 were independent and 53.5% had intensities greater than 2σ(F^2) [23]. A multiscan absorption correction was applied using SADABS 2016/2 [24]. The structure was solved using intrinsic phasing methods using SHELXT 2018/2 and refined by full-matrix least squares methods against F^2 using SHELXL-2019/2 [25,26]. The molecular model of the title compound was drawn using ORTEP-3 software for windows [27]. The software used for the illustration of the structure and crystallographic parameters was Mercury (CCDC) [28,29] and PLATON [30].

The refinement details and crystal structure data are listed in Table 1. The refinement of all non-hydrogen atoms was done anisotropically, and the positions of hydrogen atoms were determined based on Fourier difference electron density maps. The refinement of all CH's and aromatic hydrogen atoms (C-H = 0.95 Å) was done by using the riding model with U_{iso}(H) = 1.2 U_{eq}(C). The final least-squares refinement on F^2 congregated satisfactorily with a goodness-of-fit value of 1.006. For reflections with $I \ge 2\sigma(I)$, the reliability factors were R_1 = 0.0691 and wR_2 = 0.1431, while refinement against all data gave R_1 = 0.1488 and wR_2 = 0.1934. The largest residual electron-density peak was at 0.56 eÅ^{-3} and hole in the final difference Fourier map was at −0.60 eÅ^{-3}. An extinction coefficient of 0.0138(11) was applied during refinement.

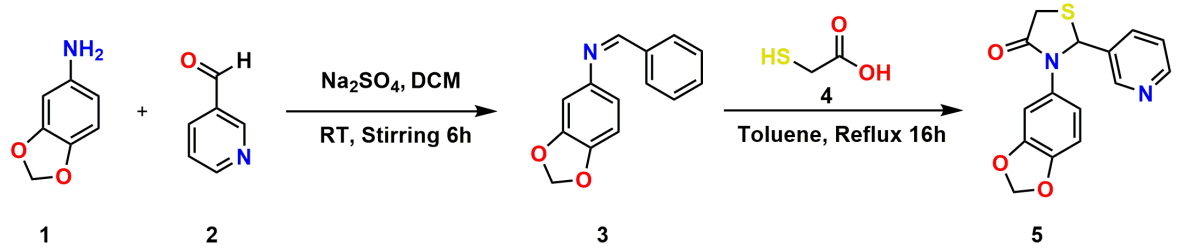

Scheme 1. Synthesis scheme of 3-(benzo[*d*][1,3]dioxol-5-yl)-2-(pyridin-3-yl)thiazolidin-4-one.

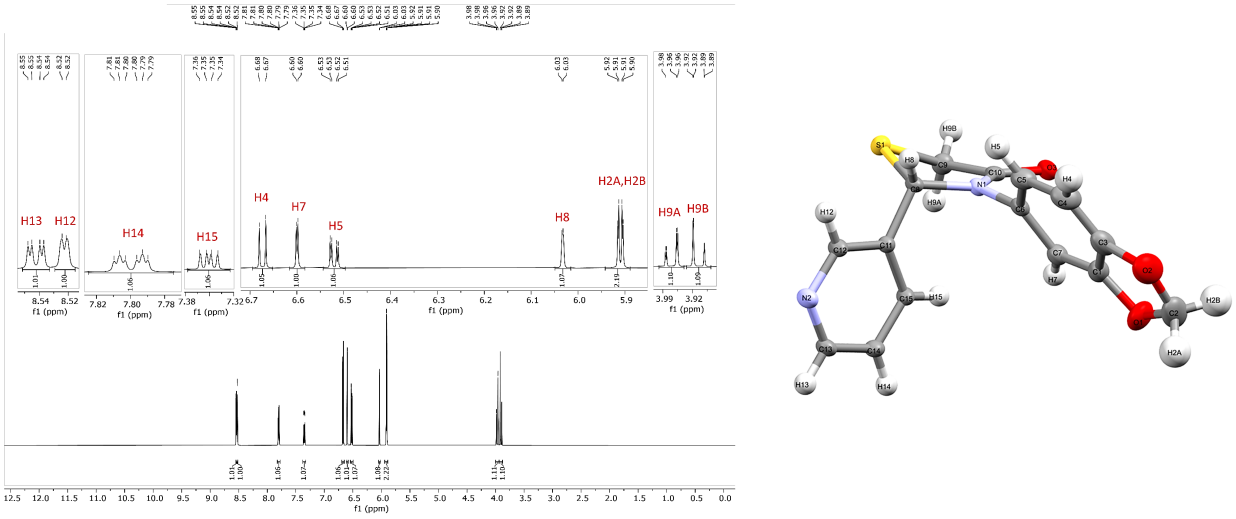

Figure 1. ^{1}H NMR spectrum of 3-(benzo[*d*][1,3]dioxol-5-yl)-2-(pyridin-3-yl)thiazolidin-4-one.

The supplementary crystallographic data for the structure reported in this study have been deposited with the Cambridge Crystallographic Data Centre [31] with CCDC number 2440462.

3. Results and discussion

3.1. Synthesis

3-(Benzo[*d*][1,3]dioxol-5-yl)-2-(pyridin-3-yl)thiazolidin-4-one (5) was synthesized by a two-step procedure. In the first step, pyridine-3-carbaldehyde (2) and benzo[d][1,3]dioxol-5-amine (1) were reacted in dichloromethane at room temperature in the presence of anhydrous Na_2SO_4 as a dehydrating agent to remove water generated during the reaction. The resulting Schiff base 3, without purification, was subsequently dissolved in toluene and refluxed with thioglycolic acid (4) for 16 h, as previously reported [32] (Scheme 1).

The construction of the heterocyclic 1,3-thiazolidin-4-one ring in the title compound was confirmed by the ^{1}H NMR spectrum. A doublet (J = 2.1 Hz) at the chemical shift of δ 6.03 ppm was assigned to one proton H8 at the stereogenic center of the ring, which agreed with chemical shifts of similar compounds [33]. The small splitting of this signal is due to the coupling with the diastereotopic proton H9B of the ring CH_2. The diastereotopic protons of 1,3-thiazolidin-4-one ring CH_2 exhibited two signals at δ 3.90 ppm for H9B and δ 3.97 ppm for H9A, each with an integration of one proton, and a coupling constant of 15.9 Hz, in line with the values given in the literature [34]. In the benzo[*d*][1,3]dioxol-5-yl group, the protons of the CH_2 group between two oxygen atoms were also diastereotopic but their chemical shifts were very close due to a larger distance from the chiral center in this case. These protons appear as doublets due to the merging of two signals with J value 12 Hz at δ 5.93-5.88 ppm. The aromatic protons of the benzo[*d*][1,3] dioxol-5-yl group appeared between δ 6.52-6.67 ppm with a characteristic splitting pattern. The aromatic protons of the pyridyl moiety resonated at a downfield multiplate at δ 7.35-8.54 ppm, with splitting patterns arising from *ortho*-, *meta*-, and *para*-coupling interactions [35] (Figure 1).

In the ^{13}C spectrum of the title compound, a signal at δ 63.3 ppm corresponds to the stereogenic carbon. The CH_2 group in the thiazolidinone ring was observed at δ 33.3 ppm, which was further corroborated by a characteristic downward peak in the DEPT-135 spectrum. In the benzo[*d*][1,3]dioxol-5-yl group, the CH_2 group between two oxygen atoms also produced a downward signal at δ 101.8 ppm in the DEPT-135 spectrum. The carbonyl carbon of the amide group appeared at δ 170.7 ppm, which is a characteristic peak for the 1,3-thiazolidin-4-one carbonyl carbon [36] (Figure 3). Signals corresponding to the aromatic ring carbons appeared between δ 107.64-149.31 ppm (Figure 2). Comparison of the broadband ^{13}C spectrum with DEPT-135 of the title compound indicated five quaternary carbons, and the DEPT-90 spectrum further confirmed nine CH signals in the molecule (Figure 3).

3.2. X-ray crystallographic analysis

Single-crystal X-ray diffraction analysis was performed for compound 5. A suitable crystal was placed on the diffractometer. The compound crystallizes in the monoclinic crystal system with space group *C*2/*c* (No. 15). The unit-cell dimensions were a = 14.69 Å, b = 9.615 Å, c = 22.198 Å, and β = 98.49° (Table 1). The crystal structure showed 3-pyridyl and benzo[*d*][1,3]dioxol-5-yl groups attached to the thiazolidine ring at 2 and 3 positions, respectively, as shown in Figure 4. The selected bond angles and bond lengths of the structure are given in Table 2.

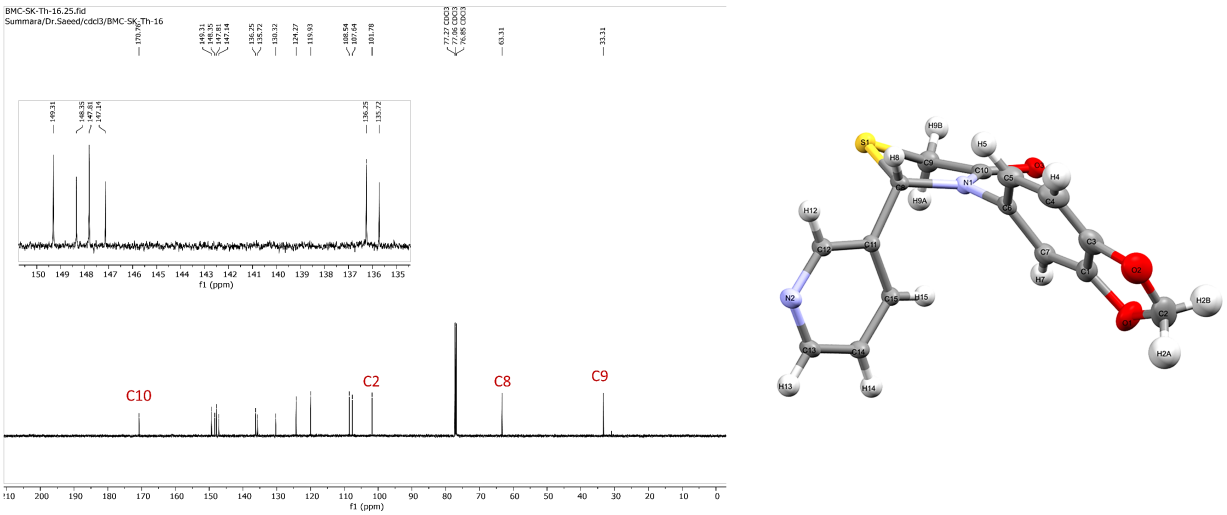

Figure 2. ^{13}C NMR spectrum of 3-(benzo[*d*][1,3]dioxol-5-yl)-2-(pyridin-3-yl)thiazolidin-4-one.

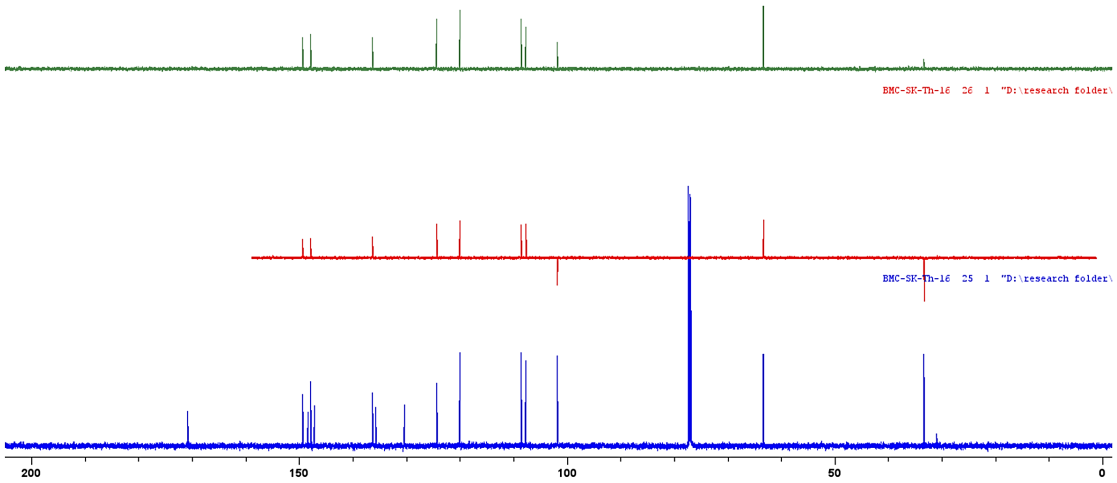

Figure 3. Stacked DEPT 90 (green), DEPT 135 (red) and broad band (blue) spectrum of 3-(benzo[*d*][1,3]dioxol-5-yl)-2-(pyridin-3-yl)thiazolidin-4-one.

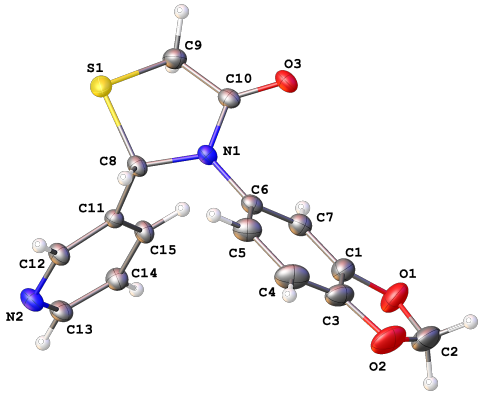

Figure 4. ORTEP view of compound **5** showing the atom-numbering scheme. Thermal ellipsoids are drawn at a 50% probability.

The angle between the planes of the 3-pyridyl and benzo[d][1,3]dioxol-5-yl rings is almost perpendicular, showing an angle equal to 88.32(5)°. In the thiazolidine ring the sulfur atom is deviated from the average plane of (C8-N1-C10-C9) by 0.529(2) Å, indicating that the five-membered ring adopts a non-planar (bent) conformation in accordance with similar reported structures [37,38]. The molecular packing in the crystal is stabilized by the three main hydrogen bonding interactions of the type C-H···O and C-H···N (Table 3). The first one is the relatively strong and directional atoms involving C8-H8···O3(1/2-*x*, 1/2+*y*, *z*) with distance equal to 2.173(1) Å and donor-acceptor (D···A) distance of 3.139(2) Å, with a bond angle of 162°, indicating a nearly linear interaction.

Table 2. Bond lengths and angles for 3-(benzo[d][1,3]dioxol-5-yl)-2-(pyridin-3-yl)thiazolidin-4-one.

Bond	Distance (Å)	Bond	Angle (°)	Bond	Angle (°)
S1-C8	1.837(2)	C8-S1-C9	92.01(8)	S1-C9-C10	105.9(1)
S1-C9	1.801(2)	C1-O1-C2	105.4(2)	N1-C10-O3	124.1(1)
O1-C1	1.371(2)	C6-N1-C8	120.6(1)	N1-C10-C9	112.1(1)
O1-C2	1.431(3)	C6-N1-C10	121.1(1)	O3-C10-C9	123.8(1)
N1-C6	1.438(2)	C8-N1-C10	118.1(1)	C8-C11-C12	118.5(1)
N1-C8	1.455(2)	O1-C1-C3	110.2(2)	C8-C11-C15	123.0(1)
N1-C10	1.358(2)	O1-C1-C7	127.4(2)	C12-C11-C15	118.4(1)
C1-C3	1.381(3)	C3-C1-C7	122.4(2)	N2-C12-C11	123.9(1)
C1-C7	1.363(2)	C2-O2-C3	105.8(2)	N2-C13-C14	123.5(2)
O2-C2	1.423(3)	C12-N2-C13	116.6(1)	C13-C14-C15	119.5(2)
O2-C3	1.373(2)	O1-C2-O2	108.5(2)	C11-C15-C14	118.1(1)
N2-C12	1.341(2)	C1-C3-O2	109.7(2)		
N2-C13	1.335(2)	C1-C3-C4	122.1(2)		
O3-C10	1.225(2)	O2-C3-C4	128.2(2)		
C3-C4	1.363(3)	C3-C4-C5	116.9(2)		
C4-C5	1.402(3)	C4-C5-C6	120.5(2)		
C5-C6	1.383(3)	N1-C6-C5	120.3(1)		
C6-C7	1.400(2)	N1-C6-C7	117.6(1)		
C8-C11	1.508(2)	C5-C6-C7	122.0(2)		
C9-C10	1.508(2)	C1-C7-C6	116.1(2)		
C11-C12	1.388(2)	S1-C8-N1	104.7(1)		
C11-C15	1.388(2)	S1-C8-N8	108.5(2)		
C13-C14	1.380(2)	S1-C8-C11	112.4(1)		
C14-C15	1.381(2)	N1-C8-C11	113.7(1)		

Table 3. Hydrogen-bond geometry in the compound 5.

No	D-H···A	D-H (Å)	H···A (Å)	D···A (Å)	∠D-H···A (°)
1	C8-H8···O3 [i]	1.00	2.17	3.139(2)	162
2	C13-H13···O3 [ii]	0.95	2.51	3.270(2)	137
3	C15-H15···N2 [iii]	0.95	2.53	3.450(2)	164

Symmetry codes: (i) 1/2-*x*, 1/2+*y*, *z*; (ii) 1/2-*x*, -1/2+*y*, *z*; (iii) 3/2-*x*, -1/2+*y*, *z*.

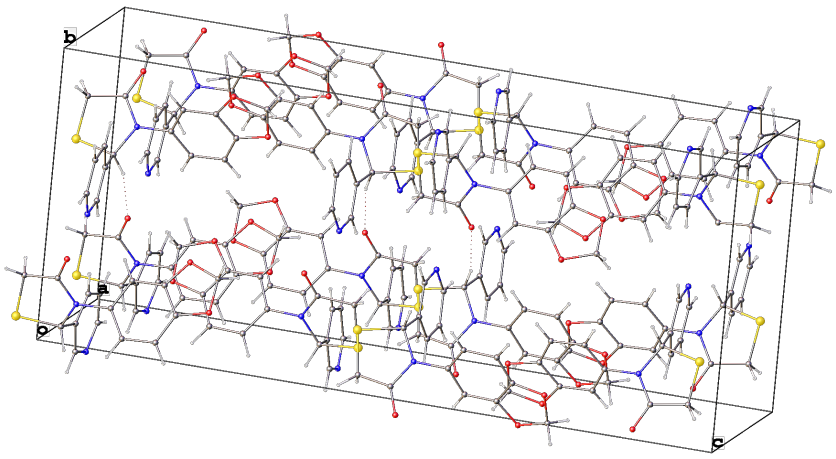

Figure 5. Crystal packing in compound **5**. C–H···O and C–H···N interactions are shown as dashed lines.

The second relatively weaker and more bent interaction is between C13-H13···O3 (1/2-*x*, -1/2+*y*, *z*) with H···O distance equal to 2.506(1) Å and D···A distance of 3.270(2) Å, with an angle of 137°. The third one is also weaker and nearly linear interaction between N2 of the pyridyl group and H15 (1/2-*x*, -1/2+*y*, +*z*) with H···N distance 2.526(2)Å and D···A distance of 3.450(2) Å, and a bond angle of 164° (Figure 5). Similar molecules containing thiazolidinone ring previously reported in the literature have shown comparable hydrogen bonding interactions [37,39]. The PLATON software package was used to analyze hydrogen bond interactions [30].

The three-dimensional crystal structure is further stabilized by weak π-π interactions involving the benzo[*d*][1,3] dioxole group of the title compound 5. The interaction is between the benzene ring of one molecule and the dioxole ring of the adjacent molecule. The dioxole ring alone is not strongly aromatic, but the fused benzo[*d*][1,3]dioxole system overall supports π interactions due to the electron density of oxygen atoms. Three types of ring centroids were identified as benzene, dioxole, and pyridine rings and labeled as A (C2-C1-C3-O2-O1), B (C7-C1-C6-C3-C5-C4), and C (C13-N2-C11-C12-C14-C15). The alternating centroids A and B of the two antiparallel stacked molecules face each other, with centroid–centroid (CgA···CgB) distances of 3.693 and 4.649 Å, which fall within or near the typical range for π-π interactions (3.3 to 4.0 Å). The interacting rings are not perfectly antiparallel, but are slightly inclined, adopting a slipped parallel stacking arrangement, with a torsion angle of 28 ° between the A-B-A-B centroids responsible for a small lateral offset (slippage). In contrast, the centroid–centroid (CgC···CgC) distance between pyridine rings of adjacent molecules is significantly longer, at 6.040 Å, indicating a much weaker or negligible contribution to π-π stacking (Figure 6). Similar π-π interaction distances have been reported in a related molecule in the literature [40]. CCDC Mercury software was used to visualize the π-π interactions in crystal packing [29].

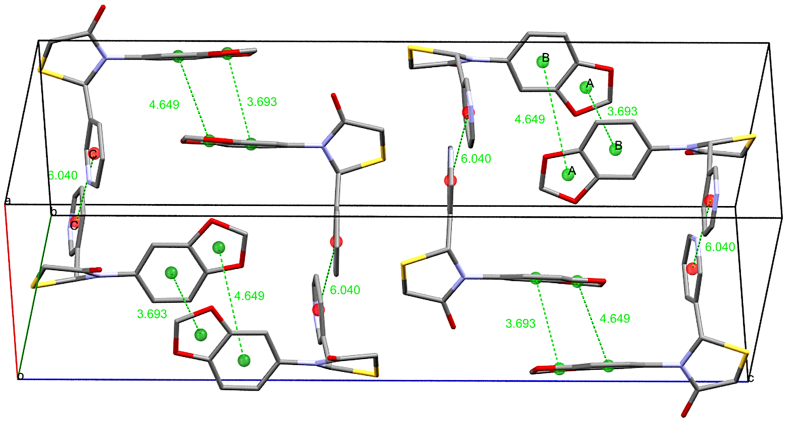

Figure 6. The π-π stacking in compound 5. The dashed lines represent the π-π interactions between the centroids of adjacent rings.

3.3. Hirshfeld surface and two-dimensional fingerprint plot analysis

A Hirshfeld surface analysis model was used to study the intermolecular interactions in the title compound and the packing of molecules in the crystal. These parameters were calculated using Crystal Explorer version 21.5 [41]. The normalized contact distance, d_{norm} is obtained by taking the normalized sum of the distances of any surface point to the nearest interior atom (d_i), the distances of any surface point to the nearest exterior atom (d_e) and the sum of van der Waals radii (vdw) of the atoms as shown in Equation 1 [42,43]. The resulting maps of these parameters are presented on the Hirshfeld surface of the title compound as shown in Figure 7.

$$d_{norm} = \frac{\{d_i - r_i^{\{vdW\}}\}}{\{r_i^{\{vdW\}}\}} + \frac{\{d_e - r_e^{\{vdW\}}\}}{\{r_e^{\{vdW\}}\}} \quad (1)$$

The three-dimensional d_{norm} surface, obtained by mapping over a fixed color -0.3929 (red) to 1.3526 (blue), explains intermolecular O···H close contacts as red spots on the surface. These red spots indicate that the sum of d_i and d_e is shorter than the sum of the van der Waals radii. On the contrary, the blue and white regions on the surface show that the sum of d_i and d_e is longer and/or equal to the sum of the van der Waals radii respectively [44] (Figure 7a-c). The Hirshfeld surface plotted with a shape index between -1 and 1, the concave red regions on the surface map denote acceptor groups and the convex blue regions denote hydrogen donor groups (Figure 7e) [45]. Electrostatic potentials for 3-(benzo[*d*][1,3]dioxol-5-yl)-2-(pyridin-3-yl)thiazolidin-4-one were also mapped on the Hirshfeld surface over the range of -0.0412 to 0.0390 atomic units [46] and were calculated using B3LYP/6-31G(d,p) level of theory [47]. The electrostatic potential map provides quantitative analysis of positive and negative potential regions in the molecule. The electron-deficient and electron rich sites in the molecule are represented as red and blue, respectively. In the title compound, the electron rich sites are around the electronegative atoms O, N, S containing groups such as carbonyl C=O of the 1,3-thiazolidin-4-one ring, and S and N atoms in the ring, as well as, around the O atoms of the 3-(benzo[*d*][1,3]dioxol-5-yl) group. Electron-deficient sites were present around the C-H bonds of the two heteroaromatic rings and the central 1,3-thiazolidin-4-one ring [39] (Figure 7d).

Hirshfeld surface analysis also provided two-dimensional (2D) fingerprint plots, which offer a quantitative explanation of the intermolecular interactions present in the crystal lattice. The overall fingerprint plot exhibits a symmetric distribution of contacts and is a plot of the distance of d_e (distance from the Hirshfeld surface to the nearest external atom) versus d_i (distance to the nearest internal atom). Each point in the fingerprint plot corresponds to a contact point on the Hirshfeld surface at a specific location. The colors in the graph represent the frequency of contacts (red = many, green = moderate, blue = few) [48]. For the title compound, H···H interactions constitute the largest contribution (32.4%) and appear as a broad central region, indicating the dominance of van der Waals interactions. The O···H/H···O contacts contribute 20.2% and are characterized by sharp spikes at low d_i and d_e values, confirming the presence of significant hydrogen bonding interactions. These hydrogen bonds originate from the carbonyl oxygen atom and the two oxygen atoms of the benzo[d][1,3]dioxol-5-yl moiety. The C···H/H···C interactions, representing 18.1%, display characteristic wing-shaped patterns, indicative of weak C–H···π interactions that contribute to the stabilization of the crystal packing. The remaining S···H/H···S (10.5%), N···H/H···N (9.4%), C···O/O···C (6.9%), C···C (1.2%), and C···N/N···C (0.2%) interactions make relatively minor contributions to the Hirshfeld surface. The low percentage of C···C contacts suggests limited π···π stacking interactions in the crystal structure. These percentages follow the same descending order (H···H to N···H) as reported for a similar compound in the literature [39] (Figures 8a-8i).

3.4. Energy framework

Interaction energies were calculated by generating a cluster of molecules within a 3.8 Å radius of the title compound in the stabilized crystal packing. For this analysis, energy theory HF/3-21G [49] in Crystal Explorer 12.5 software was used [43]. The Tonto quantum chemistry package [50] was used for wave function calculation in contrast to the Gaussian 16 software package [51] because Tonto is optimized specifically for crystallographic and wave function-based analyses and can access the static electron densities in the solid crystal to accurately evaluate intermolecular interactions. In contrast, Gaussian 16 is designed for quantum chemical calculations of isolated molecules or in gas phase without crystal-packing effects [52].

The interaction energies are illustrated in the form of graphs in Figure 9 using energy representations. The thickness of the colored cylinders is directly proportional to the extent of interaction energy. The total intermolecular energy E_{tot} (kJ/mol) of the title compound (represented as gray ball and stick model) is comprised of four main component energies, dispersion (E_{dis}), polarization (E_{pol}), exchange-repulsion (E_{rep}), and electrostatic (E_{ele}) [53] with scale factors of 0.871, 0.740, 0.618 and 1.057, respectively [49,54].

Table 4. Component-wise intermolecular interaction energies for 3-(benzo[*d*][1,3]dioxol-5-yl)-2-(pyridin-3-yl)thiazolidin-4-one.

Color	N	Symop	R	E_{ele}	E_{pol}	E_{dis}	E_{rep}	E_{tot}
	2	*x*, *y*, *z*	7.90	-3.6	-2.9	-24.8	14.2	-16.4
	2	*x*+1/2, *y*, -*z*+1/2	7.48	-7.1	-3.6	-39.8	15.8	-32.6
	2	-*x*+1/2, *y*+1/2, *z*	7.36	-26.8	-9.0	-27.6	21.4	-40.6
	1	-*x*, -*y*, -*z*	9.75	-1.7	-0.6	-9.8	4.1	-7.7
	2	*x*+1/2, -*y*+1/2, -*z*	8.76	-13.5	-2.3	-27.3	19.7	-23.9
	2	-*x*, *y*+1/2, -*z*+1/2	8.75	1.2	-1.7	-14.9	4.0	-10.1
	2	-*x*+1/2, *y*+1/2, *z*	7.03	-27.3	-9.0	-20.3	19.0	-36.6
	1	-*x*, -*y*, -*z*	9.97	1.9	-0.3	-2.7	0.0	-0.7
Total				-76.9	-29.4	-167.2	98.2	-168.6

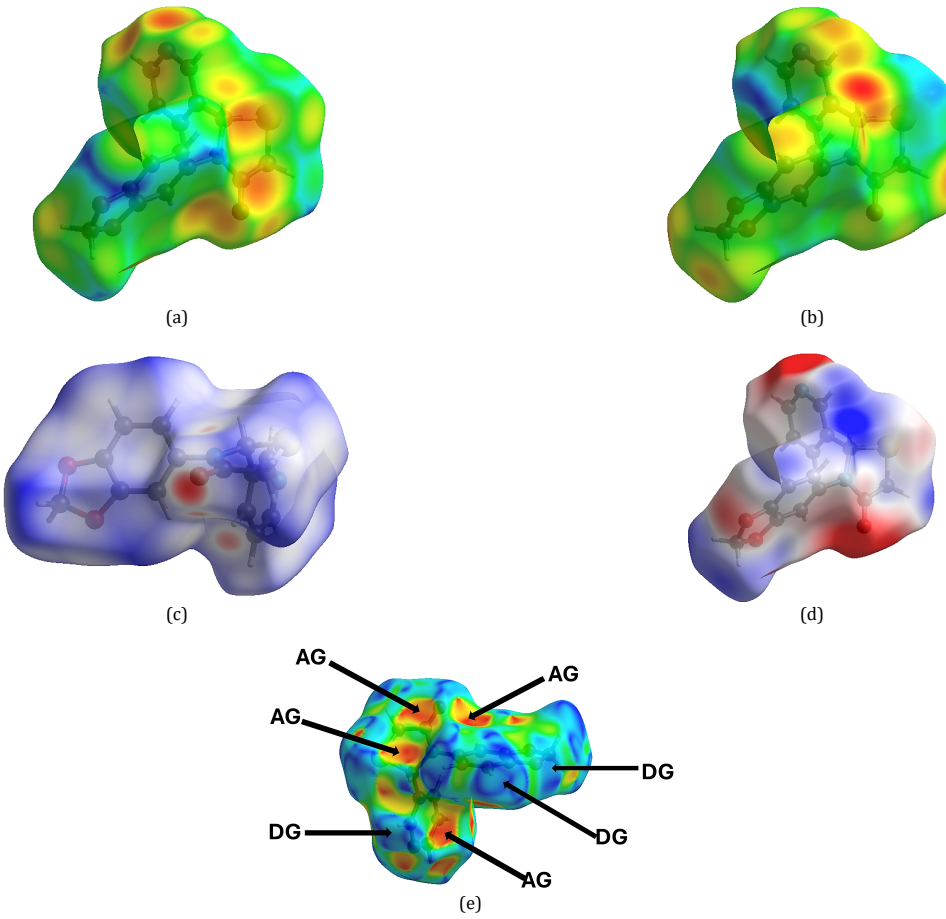

Figure 7. The Hirshfeld surface of the compound plotted over: (a) d_e in the range 0.8833 to 2.6413 Å, (b) d_i in the range 0.8837 to 2.7999 Å, (c) d_{norm} in the range -0.3929 to 1.3520, (d) electrostatic potential in the range -0.0412 to 0.0390 atomic units. (e) shape-index (-1.0 to 1.0, AG: Acceptor Group, DG: Donor Group).

Additional interaction energy parameters obtained include rotational symmetry operations (SymOp) relative to the central molecule, the number of interacting molecular pairs (N), and the centroid–centroid distances (R) between the central molecule and its interacting counterparts. The intermolecular interaction energy analysis shows that the crystal packing of the title compound is extensively stabilized by non-directional dispersion interactions as reflected by its large magnitude of -167.2 kJ/mol, which is mainly due to C–H···π interactions involving the benzo[*d*][1,3]dioxole and pyridyl moieties and the π–π interactions between aromatic rings. The significant electrostatic or Coulombs energy contribution (-76.9 kJ/mol) can be credited to the presence of weak hydrogen-bonding interactions, mainly C–H···O and C–H···N contacts involving the carbonyl oxygen, heterocyclic sulfur, and pyridine nitrogen atoms. The polarization energy contribution of -29.4 kJ/mol further supports the involvement of these heteroatoms, indicating electronic distortion between interacting molecules. All of these attractive contributions are partially compensated for by the repulsion energy of +98.2 kJ/mol, which arises from closely packed regions of the crystal involving short-range electron density overlap. In general, the sum of these interactions results in a stabilizing total interaction energy of -168.6 kJ/mol (Table 4). The dominance of dispersion interactions is also reflected in the corresponding energy framework diagram with thick cylinders observed for the dispersion energy components, as described in the literature for a similar compound [39] (Figures 9c and 9d).

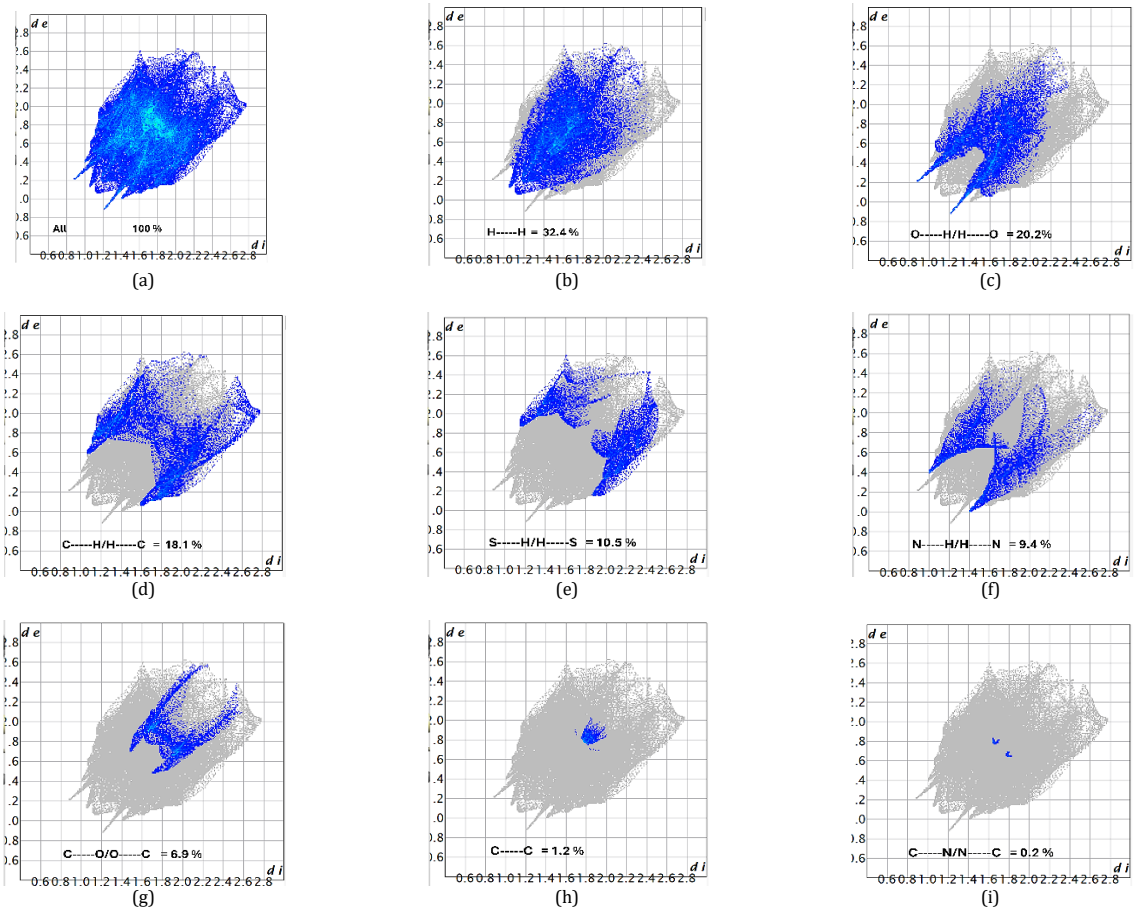

Figure 8. Two-dimensional fingerprint plots of title compound showing contributions from: (a) all intermolecular contacts, (b) H···H (c) O···H/H···O, (d) C···H/H···C, (e) S···H/H···S, (f) N···H/H···N, (g) C···O/O···C, (h) C···C, (i) C···N/N···C.

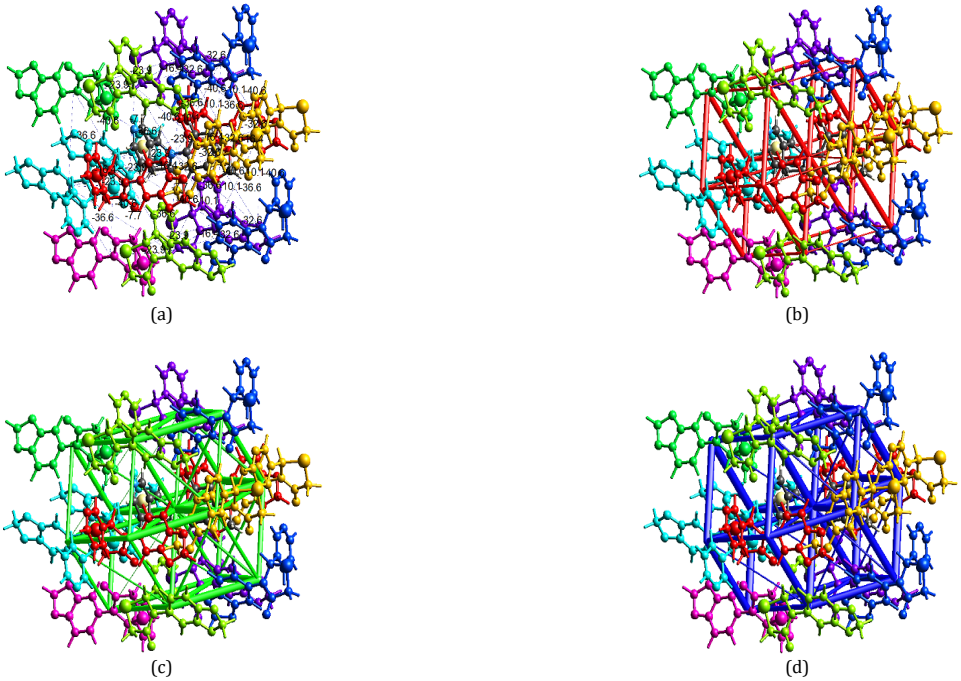

Figure 9. Color-coded interaction energy framework map of 3-(benzo[*d*][1,3]dioxol-5-yl)-2-(pyridin-3-yl)thiazolidin-4-one for interactions within 3.8 Å of the central gray ball-and-stick molecule (a). Energy framework diagram for the Coulomb energy (b), the dispersion energy of the title compound (c), and the total interaction energy (d). Energy framework calculations were performed at the HF/3-21G level of theory, employing a scale factor of 100 and an interaction energy cut-off value of 5.00 kJ/mol.

4. Conclusions

A novel 1,3-thiazolidin-4-one derivative, 3-(benzo[*d*][1,3]dioxol-5-yl)-2-(pyridin-3-yl)thiazolidin-4-one, was successfully synthesized and comprehensively characterized using spectroscopic techniques and single-crystal X-ray diffraction. The crystallographic analysis revealed a non-planar thiazolidine ring conformation and confirmed the molecular geometry. Detailed exploration of the crystal packing demonstrated that the solid-state structure is stabilized by a mixture of hydrogen bonding and weak π···π interactions. The Hirshfeld surface and energy framework analyses provided quantitative understanding of intermolecular contacts and established that dispersion forces play a dominant role in stabilizing the crystal lattice. These structural and intermolecular interaction characteristics contribute to a deeper understanding of the solid-state behavior of this 1,3-thiazolidin-4-one scaffold and may be valuable for future studies of structure-property and structure-activity relationships.

Acknowledgements

This work was supported by internal funding awarded to Muhammad Saeed from the Lahore University of Management Sciences under Faculty Initiative Funds (FIF-0918/CH).

Supporting information

CCDC-2440462 contains the supplementary crystallographic data for this article. These data can be obtained free of charge via www.ccdc.cam.ac.uk/data request/cif, or by e-mailing data request@ccdc.cam.ac.uk, or by contacting The Cambridge Crystallographic Data Centre, 12 Union Road, Cambridge CB2 1EZ, UK; fax: +44(0)1223-336033.

CRediT authorship contribution statement

Conceptualization: Muhammad Saeed, Monther Khanfar, Summara Kousar; Methodology: Muhammad Saeed, Summara Kousar; Software: Raed Al-Qawasmeh, Monther Khanfar; Validation: Muhammad Saeed, Raed Al-Qawasmeh, Monther Khanfar; Resources: Muhammad Saeed, Monther Khanfar; Data Curation: Summara Kousar, Raed Al-Qawasmeh; Writing - Original Draft: Summara Kousar; Writing - Review and Editing: Summara Kousar, Muhammad Saeed; Visualization: Summara Kousar, Raed Al-Qawasmeh, Monther Khanfar; Funding acquisition: Muhammad Saeed; Supervision: Muhammad Saeed; Project Administration: Muhammad Saeed.

Disclosure statement

Ethical approval: All relevant ethical standards were strictly followed.
Conflict of interest: The authors declare that there are no competing interests.
Sample availability: Samples of the compound can be available from the authors upon request.

Funding

This work was supported by Faculty Initiative Funds (FIF-0918/CH).

ORCID and Email

Summara Kousar
21130019@lums.edu.pk
https://orcid.org/0009-0002-4609-0366
Read Al-Qawasmeh
ralqawasmeh@sharjah.ac.ae
https://orcid.org/0000-0002-9325-6229
Monther Khanfar
mkhanfar@sharjah.ac.ae
https://orcid.org/0000-0003-4718-4006
Muhammad Saeed
muhammad.saeed@lums.edu.pk
https://orcid.org/0000-0002-9229-838X

References

[1]. Kabir, E.; Uzzaman, M. A review on biological and medicinal impact of heterocyclic compounds. *Results Chem.* **2022**, *4*, 100606.
[2]. Brown, F. C. 4-Thiazolidinones. *Chem. Rev.* **1961**, *61* (5), 463–521.
[3]. Jain, A. K.; Vaidya, A.; Ravichandran, V.; Kashaw, S. K.; Agrawal, R. K. Recent developments and biological activities of thiazolidinone derivatives: A review. *Bioorg. Med. Chem.* **2012**, *20* (11), 3378–3395.
[4]. Patel, D.; Kumari, P.; Patel, N. Synthesis and biological evaluation of some thiazolidinones as antimicrobial agents. *Eur. J. Med. Chem.* **2012**, *48*, 354–362.
[5]. Goel, B.; Ram, T.; Tyagi, R.; Bansal, E.; Kumar, A.; Mukherjee, D.; Sinha, J. N. 2-Substituted-3-(4-bromo-2-carboxyphenyl)-5-methyl-4-thiazolidinones as potential anti-inflammatory agents. *Eur. J. Med. Chem.* **1999**, *34*, 265–269.
[6]. Hu, J.; Wang, Y.; Wei, X.; Wu, X.; Chen, G.; Cao, G.; Shen, X.; Zhang, X.; Tang, Q.; Liang, G.; Li, X. Synthesis and biological evaluation of novel thiazolidinone derivatives as potential anti-inflammatory agents. *Eur. J. Med. Chem.* **2013**, *64*, 292–301.
[7]. Moreira, D. R.; Lima Leite, A. C.; Cardoso, M. V.; Srivastava, R. M.; Hernandes, M. Z.; Rabello, M. M.; da Cruz, L. F.; Ferreira, R. S.; de Simone, C. A.; Meira, C. S.; Guimaraes, E. T.; da Silva, A. C.; dos Santos, T. A.; Pereira, V. R.; Pereira Soares, M. B. Structural Design, Synthesis and Structure–Activity Relationships of Thiazolidinones with Enhanced Anti-*Trypanosoma cruzi* Activity. *ChemMedChem* **2013**, *9* (1), 177–188.
[8]. de Oliveira Filho, G. B.; de Oliveira Cardoso, M. V.; Espíndola, J. W.; Ferreira, L. F.; de Simone, C. A.; Ferreira, R. S.; Coelho, P. L.; Meira, C. S.; Magalhaes Moreira, D. R.; Soares, M. B.; Lima Leite, A. C. Structural design, synthesis and pharmacological evaluation of 4-thiazolidinones against Trypanosoma cruzi. *Bioorg. Med. Chem.* **2015**, *23* (23), 7478–7486.
[9]. Gamal, M. A.; Fahim, S. H.; Giovannuzzi, S.; Fouad, M. A.; Bonardi, A.; Gratteri, P.; Supuran, C. T.; Hassan, G. S. Probing benzenesulfonamide–thiazolidinone hybrids as multitarget directed ligands for efficient control of type 2 diabetes mellitus through targeting the enzymes: α-glucosidase and carbonic anhydrase II. *Eur. J. Med. Chem.* **2024**, *271*, 116434.
[10]. Saeedian Moghadam, E.; Sameem, B.; Abdel-Jalil, R.; Faramarzi, M. A.; Amini, M. 5-Benzylidene-2,3-diarylthiazolidine-4-ones: Design, synthesis, spectroscopic characterization, *in vitro* biological and computational evaluation. *Synth. Commun.* **2021**, *51* (17), 2668–2683.
[11]. Barbosa, V. A.; Baréa, P.; Mazia, R. S.; Ueda-Nakamura, T.; Costa, W. F.; Foglio, M. A.; Goes Ruiz, A. L.; Carvalho, J. E.; Vendramini–Costa, D. B.; Nakamura, C. V.; Sarragiotto, M. H. Synthesis and evaluation of novel hybrids β -carboline-4-thiazolidinones as potential antitumor and antiviral agents. *Eur. J. Med. Chem.* **2016**, *124*, 1093–1104.
[12]. Chen, H.; Yang, T.; Wei, S.; Zhang, H.; Li, R.; Qin, Z.; Li, X. Synthetic bicyclic iminosugar derivatives fused thiazolidin-4-one as new potential HIV-RT inhibitors. *Bioorg. Med. Chem. Lett.* **2012**, *22* (23), 7041–7044.
[13]. Cheddie, A.; Shintre, S. A.; Bantho, A.; Mocktar, C.; Koorbanally, N. A. Synthesis and antibacterial activity of a series of 2-trifluoromethylbenzimidazole-thiazolidinone derivatives. *J. Heterocycl. Chem.* **2019**, *57* (1), 299–307.
[14]. Cascioferro, S.; Parrino, B.; Carbone, D.; Schillaci, D.; Giovannetti, E.; Cirrincione, G.; Diana, P. Thiazoles, Their Benzofused Systems, and Thiazolidinone Derivatives: Versatile and Promising Tools to Combat Antibiotic Resistance. *J. Med. Chem.* **2020**, *63* (15), 7923–7956.
[15]. Singh, N.; Agarwal, R. C.; Singh, C. P. Synthesis and Evaluation of Some Substituted Indole Derivatives for Cardiovascular Activity. *Int. J. Pharm. Sci. Drug Res.* **2018**, 14–17.
[16]. Ottanà, R.; Carotti, S.; Maccari, R.; Landini, I.; Chiricosta, G.; Caciagli, B.; Vigorita, M. G.; Mini, E. In vitro antiproliferative activity against human colon cancer cell lines of representative 4-thiazolidinones. Part I. *Bioorg. Med. Chem. Lett.* **2005**, *15* (17), 3930–3933.
[17]. Havrylyuk, D.; Zimenkovsky, B.; Vasylenko, O.; Gzella, A.; Lesyk, R. Synthesis of New 4-Thiazolidinone-, Pyrazoline-, and Isatin-Based Conjugates with Promising Antitumor Activity. *J. Med. Chem.* **2012**, *55* (20), 8630–8641.
[18]. Nirwan, S.; Chahal, V.; Kakkar, R. Thiazolidinones: Synthesis, Reactivity, and Their Biological Applications. *J. Heterocycl. Chem.* **2019**, *56* (4), 1239–1253.
[19]. Bolla, G.; Sarma, B.; Nangia, A. K. Crystal Engineering of Pharmaceutical Cocrystals in the Discovery and Development of Improved Drugs. *Chem. Rev.* **2022**, *122* (13), 11514–11603.
[20]. Desiraju, G. R. Crystal Engineering: From Molecule to Crystal. *J. Am. Chem. Soc.* **2013**, *135* (27), 9952–9967.
[21]. Hamdani, S. S.; Khan, B. A.; Hameed, S.; Batool, F.; Saleem, H. N.; Mughal, E. U.; Saeed, M. Synthesis and evaluation of novel S-benzyl- and S-alkylphthalimide- oxadiazole -benzenesulfonamide hybrids as inhibitors of dengue virus protease. *Bioorg. Chem.* **2020**, *96*, 103567.

[22]. Batool, F.; Saeed, M.; Saleem, H. N.; Kirschner, L.; Bodem, J. Facile Synthesis and In Vitro Activity of N-Substituted 1,2-Benzisothiazol-3(2H)-ones against Dengue Virus NS2BNS3 Protease. *Pathogens* **2021**, *10* (4), 464.
[23]. Bruker (2008). SAINT. Bruker AXS Inc., Madison, Wisconsin, USA.
[24]. Krause, L.; Herbst-Irmer, R.; Sheldrick, G. M.; Stalke, D. Comparison of silver and molybdenum microfocus X-ray sources for single-crystal structure determination. *J. Appl. Crystallogr.* **2015**, *48* (1), 3–10.
[25]. Sheldrick, G. M. *SHELXT*– Integrated space-group and crystal-structure determination. *Acta. Crystallogr. A. Found. Adv.* **2015**, *71* (1), 3–8.
[26]. Sheldrick, G. M. Crystal structure refinement with *SHELXL*. *Acta. Crystallogr. C. Struct. Chem.* **2015**, *71* (1), 3–8.
[27]. Farrugia, L. J. *ORTEP*-3 for Windows - a version of *ORTEP*-III with a Graphical User Interface (GUI). *J. Appl. Crystallogr.* **1997**, *30* (5), 565–565.
[28]. Macrae, C. F.; Edgington, P. R.; McCabe, P.; Pidcock, E.; Shields, G. P.; Taylor, R.; Towler, M.; van de Streek, J. *Mercury*: visualization and analysis of crystal structures. *J. Appl. Crystallogr.* **2006**, *39* (3), 453–457.
[29]. Macrae, C. F.; Sovago, I.; Cottrell, S. J.; Galek, P. T. A.; McCabe, P.; Pidcock, E.; Platings, M.; Shields, G. P.; Stevens, J. S.; Towler, M.; Wood, P. A. Mercury 4.0: from visualization to analysis, design and prediction. *J. Appl. Crystallogr.* **2020**, *53*, 226–235.
[30]. Spek, A. L. Structure validation in chemical crystallography. *Acta. Crystallogr. D. Biol. Crystallogr.* **2009**, *65* (2), 148–155.
[31]. Groom, C. R.; Bruno, I. J.; Lightfoot, M. P.; Ward, S. C. The Cambridge Structural Database. *Acta. Crystallogr. B. Struct. Sci. Cryst. Eng. Mater.* **2016**, *72* (2), 171–179.
[32]. Barreca, M. L.; Chimirri, A.; De Luca, L.; Monforte, A. M.; Monforte, P.; Rao, A.; Zappalà, M.; Balzarini, J.; De Clercq, E.; Pannecouque, C.; Witvrouw, M. Discovery of 2,3-diaryl-1,3-thiazolidin-4-ones as potent anti-HIV-1 agents. *Bioorg. Med. Chem. Lett.* **2001**, *11*, 1793–1796.
[33]. Foroughifar, N.; Ebrahimi, S. One-pot synthesis of 1,3-thiazolidin-4-one using Bi(SCH2COOH)3 as catalyst. *Chinese. Chemical. Letters.* **2013**, *24* (5), 389–391.
[34]. Elkanzi, N. A.; Bakr, R. B. Optimization of 1,3-thiazolidin-4-one based compounds: Design, synthesis, biological evaluation, molecular modeling and ADME studies. *J. Indian Chem. Soc.* **2025**, *102* (5), 101693.
[35]. Barreca, M. L.; Balzarini, J.; Chimirri, A.; Clercq, E. D.; Luca, L. D.; Höltje, H. D.; Höltje, M.; Monforte, A. M.; Monforte, P.; Pannecouque, C.; Rao, A.; Zappalà, M. Design, Synthesis, Structure−Activity Relationships, and Molecular Modeling Studies of 2,3-Diaryl-1,3-thiazolidin-4-ones as Potent Anti-HIV Agents. *J. Med. Chem.* **2002**, *45* (24), 5410–5413.
[36]. War, J. A.; Srivastava, S. K. Rationale design and synthesis of some novel imidazole linked thiazolidinone hybrid molecules as DNA minor groove binders. *Eur. J. Chem.* **2020**, *11* (2), 120–132.
[37]. Fun, H.; Hemamalini, M.; Shanmugavelan, P.; Ponnuswamy, A.; Jagatheesan, R. 3-Benzyl-2-phenyl-1,3-thiazolidin-4-one. *Acta. Crystallogr. E. Struct. Rep. Online.* **2011**, *67* (10), o2706–o2706.
[38]. Gzella, A. K.; Kowiel, M.; Suseł, A.; Wojtyra, M. N.; Lesyk, R. Heterocyclic tautomerism: reassignment of two crystal structures of 2-amino-1,3-thiazolidin-4-one derivatives. *Acta. Crystallogr. C. Struct. Chem.* **2014**, *70* (8), 812–816.
[39]. Abdel-Rahman, L. H.; Mohamed, S. K.; El Bakri, Y.; Ahmad, S.; Lai, C.; Amer, A. A.; Mague, J. T.; Abdalla, E. M. Synthesis, crystal structural determination and in silco biological studies of 3,3′-ethane-1,2-diylbis(2-benzylidene-1,3-thiazolidin-4-one. *Journal. of. Molecular. Structure.* **2021**, *1245*, 130997.
[40]. Rahmani, R.; Djafri, A.; Daran, J.; Djafri, A.; Chouaih, A.; Hamzaoui, F. Crystal structure of (2*Z*,5*Z*)-3-(4-methoxyphenyl)-2-[(4-methoxyphenyl)imino]-5-[(*E*)-3-(2-nitrophenyl)allylidene]-1,3-thiazolidin-4-one. *Acta. Crystallogr. E. Cryst. Commun.* **2016**, *72* (2), 155–157.
[41]. Spackman, M. A.; Jayatilaka, D. Hirshfeld surface analysis. *CrystEngComm.* **2009**, *11* (1), 19–32.
[42]. Seth, S. K. Structural characterization and Hirshfeld surface analysis of a Co^{II} complex with imidazo[1,2-*a*]pyridine. *Acta. Crystallogr. E. Cryst. Commun.* **2018**, *74* (5), 600–606.
[43]. Spackman, P. R.; Turner, M. J.; McKinnon, J. J.; Wolff, S. K.; Grimwood, D. J.; Jayatilaka, D.; Spackman, M. A. *CrystalExplorer*: a program for Hirshfeld surface analysis, visualization and quantitative analysis of molecular crystals. *J. Appl. Crystallogr.* **2021**, *54* (3), 1006–1011.
[44]. Vu Quoc, T.; Nguyen Ngoc, L.; Do Ba, D.; Pham Chien, T.; Nguyen Huy, H.; Van Meervelt, L. Crystal structure and Hirshfield surface analysis of 4-phenyl-3-(thiophen-3-ylmethyl)-1*H*-1,2,4-triazole-5(4*H*)-thione. *Acta. Crystallogr. E. Cryst. Commun.* **2018**, *74* (6), 812–815.
[45]. Etse, K. S.; Lamela, L. C.; Zaragoza, G.; Pirotte, B. Synthesis, crystal structure, Hirshfeld surface and interaction energies analysis of 5-methyl-1,3-bis(3-nitrobenzyl)pyrimidine-2,4(1H,3H)-dione. *Eur. J. Chem.* **2020**, *11*, 91–99.
[46]. McKinnon, J. J.; Jayatilaka, D.; Spackman, M. A. Towards quantitative analysis of intermolecular interactions with Hirshfeld surfaces. *Chem. Commun.* **2007**, 3814–3816.
[47]. Gumus, I.; Solmaz, U.; Gonca, S.; Arslan, H. Molecular self-assembly in indole-based benzamide derivative: Crystal structure, Hirshfeld surfaces and antimicrobial activity. *Eur. J. Chem.* **2017**, *8* (4), 349–357.
[48]. Chandramohan, U. M.; Joseph, D. Hirshfeld surface, fukui function, molecular docking, molecular dynamics investigation on human immunodeficiency virus-1 (HIV) organism with 2,6-dibromo-4-chloroaniline. *Results Chem.* **2024**, *11*, 101815.
[49]. Tan, S. L.; Jotani, M. M.; Tiekink, E. R. Utilizing Hirshfeld surface calculations, non-covalent interaction (NCI) plots and the calculation of interaction energies in the analysis of molecular packing. *Acta. Crystallogr. E. Cryst. Commun.* **2019**, *75* (3), 308–318.
[50]. Jayatilaka, D.; Grimwood, D. J. Tonto: A FORTRAN based object-oriented system for quantum chemistry and crystallography. In Lecture Notes in Computer Science; Springer Berlin Heidelberg: Berlin, Heidelberg, 2003; pp. 142–151.
[51]. Frisch, M. J.; Trucks, G. W.; Schlegel, H. B.; Scuseria, G. E.; Robb, M. A.; Cheeseman, J. R.; Montgomery, J. A.; Vreven, T.; Kudin, K. N.; Burant, J. C.; Millam, J. M.; Iyengar, S. S.; Tomasi, J.; Barone, V.; Mennucci, B.; Cossi, M.; Scalmani, G.; Rega, N.; Petersson, G. A.; Nakatsuji, H.; Hada, M.; Ehara, M.; Toyota, K.; Fukuda, R.; Hasegawa, J.; Ishida, M.; Nakajima, T.; Honda, Y.; Kitao, O.; Nakai, H.; Klene, M.; Li, X.; Knox, J. E.; Hratchian, H. P.; Cross, J. B.; Adamo, C.; Jaramillo, J.; Gomperts, R.; Stratmann, R. E.; Yazyev, O.; Austin, A. J.; Cammi, R.; Pomelli, C.; Ochterski, J. W.; Ayala, P. Y.; Morokuma, K.; Voth, G. A.; Salvador, P.; Dannenberg, J. J.; Zakrzewski, V. G.; Dapprich, S.; Daniels, A. D.; Strain, M. C.; Farkas, O.; Malick, D. K.; Rabuck, A. D.; Raghavachari, K; Foresman, J. B.; Ortiz, J. V.; Cui, Q.; Baboul, A. G.; Clifford, S.; Cioslowski, J.; Stefanov, B. B.; Liu, G.; Liashenko, A.; Piskorz, P.; Komaromi, I.; Martin, R. L.; Fox, D. J.; Keith, T.; Al-Laham, M. A.; Peng, C. Y.; Nanayakkara, A.; Challacombe, M.; Gill, P. M. W.; Johnson, B.; Chen, W.; Wong, M. W.; Gonzalez, C.; Pople, J. A. Gaussian 16. Gaussian, Inc., Wallingford CT, 2016.
[52]. Sieffert, N.; Wipff, G. Uranyl extraction by N,N-dialkylamide ligands studied using static and dynamic DFT simulations. *Dalton Trans.* **2015**, *44*, 2623–2638.
[53]. Turner, M. J.; Thomas, S. P.; Shi, M. W.; Jayatilaka, D.; Spackman, M. A. Energy frameworks: insights into interaction anisotropy and the mechanical properties of molecular crystals. *Chem. Commun.* **2015**, *51* (18), 3735–3738.
[54]. Mackenzie, C. F.; Spackman, P. R.; Jayatilaka, D.; Spackman, M. A. *CrystalExplorer*model energies and energy frameworks: extension to metal coordination compounds, organic salts, solvates and open-shell systems. *IUCrJ.* **2017**, *4* (5), 575–587.